CITES-2019 (27 May - 6 June 2019, Moscow, Russia
Session 1. Subeasonal and long-term meteorological and climatic predictions.

On interaction between variability mean flow and eddies and systematic errors in models

V. Krupchatnikov, Yu. Martynova, I. Borovko, G. Platov

Outline

- Introduction
- Model forecast errors: random errors, systematic errors
- Diagnosing the causes of bias in climate models
- CONCLUSIONS AND WAYS FORWARD

Acknowledgments. This work is supported by RFBR grants № 17-05-00382

By the grace of G-d

Introduction

A large number of topics have been devoted to the researches (Charney, J., M.Stern, 1962; Andrews,D., M. E. McIntyre, 1976;Simmons, A., B.Hoskins, 1978; Hoskins, B., I.James, G.White, 1983; etc.) of the interaction between vortices of various scales (from planetary to synoptic), but so far these processes are not completely clear and are under intensive research (Kaspi,Y., T.Schneider, 2013; Thompson, D.J., Y.Li, 2015;Simpson, I., T.Shaw, and R.Seager, 2014; Martynova Yu., V. Krupchatnikov, 2015; Borovko I., V. Krupchatnikov, 2015; etc.) to understand mechanisms of variability, especially the location and *strength of jets, storm tracks, blocking episodes and the sources of systematic errors in models.*

FIFTH WORKSHOP ON SYSTEMATIC ERRORS IN WEATHER AND CLIMATE MODELS 19–23 June 2017, Montreal, Quebec, Canada

The program was organized around six themes:

- the coupled atmosphere–land–ocean–cryosphere system;
- errors in the representation of clouds and precipitation;
- resolution issues, including the representation of processes in the so-called gray zones;
- model errors in ensembles;
- errors in the simulation of teleconnections between the high/midlatitudes and tropics;

WGNE - *Working Group on Numerical Experimentation*

5th WGNE Workshop on Systematic Errors (WSE)

Zadra et al. (2017) Systematic Errors in Weather and Climate Models: Nature, Origins, and Way Forward. BAMS. https://doi.org/10.1175/BAMS-D-17-0287.1

Themes:

Atmosphere-land-ocean-cryosphere interactions: errors in the representation of surface fluxes and drag processes; stable boundary layer issues; impact of coupled modeling.

Clouds and precipitation: cloud-radiative feedback problem; tropical convection issues; representation of low clouds, especially at high latitudes; excess low accumulations of precipitation; underestimation of precipitation extremes; summer continental precipitation; precipitation over orography.

Resolution issues: dependence of systematic errors on model resolution; grey zones of physical parametrizations.

Teleconnections: errors in the simulation of interactions between high-latitudes, mid-latitudes and tropics.

Metrics and diagnostics: emphasis on novel techniques (e.g. process-based diagnostics; use of data assimilation or coupled modeling) to diagnose and measure systematic errors.

Model errors in ensembles: characterization of ensemble spread and identification of systematic errors in multi-model ensembles and ensemble prediction systems; evaluation of stochastic representations.

WMO IOC ICSU International Council for Science WORLD METEOROLOGICAL ORGANIZATION WCRP World Climate Research Programme

All model evaluation efforts reveal differences when compared to observations. These differences may reflect observational uncertainty, internal variability, or errors/biases in the representation of physical processes:

• convective precipitation—the organization of convective systems; precipitation intensity and distribution; and the relationship with column-integrated water vapor, SST, and vertical velocity;
• cloud microphysics—errors linked to mixed-phase, supercooled liquid cloud, and warm rain;
• precipitation over orography—spatial distribution and intensity errors;
• MJO modeling—propagation, response to mean errors, and teleconnections;
• double intertropical convergence zone/biased ENSO—a complex combination of westward ENSO overextension, cloud–ocean interaction, and representation of tropical instability waves (TIW);
• tropical cyclones—high-resolution forecasts tend to produce cyclones that are too intense, although moderate improvements are seen from ocean coupling; wind–pressure relationship errors are systematic;
• systematic errors in the representation of heterogeneity of soil;
• stochastic physics—current schemes, while beneficial, do not necessarily/sufficiently capture all aspects of model uncertainty;
• outstanding errors in the modeling of surface fluxes; errors in the representation of the diurnal cycle of surface temperature;
• challenges in the prediction of midlatitude synoptic regimes and blocking;
• model errors in the representation of teleconnections through inadequate stratosphere–troposphere coupling; and
• model biases in mean state, diabatic heating, SST; errors in meridional wind response and tropospheric jet stream impact simulations of teleconnections.

1. Model forecast errors: random errors, systematic errors.

The precision of numerical weather prediction models is limited by errors in the model forecasts resulting from the errors in initial conditions and model deficiencies. Model forecast errors can be classified into random errors, whose time average is zero, and systematic errors.

Let us define forecast error as the difference between a model forecast *Vf* and a verifying analysis assumed to represent the "truth" *Vt*, and separate the **mean square error** into the systematic and random components:

$$\overline{(V_f - V_t)^2} = (\overline{V_f} - \overline{V_t})^2 + \overline{(V_f^{'} - V_t^{'})^2}$$

$$sfe = \overline{V_f} - \overline{V_t}$$

Systematic forecast errors *(sfes)* are a significant portion of the total forecast error in weather prediction models, such as the Global Forecast System (**gfs**), COSMO regional forecast system (**cosmo**), SLAVE forecast system (**slave**), UKMO forecast system (**ukmo**). Figures shows that after 36 houres, the amplitude of surface temperature systematic errors reach ~ 3-5C. Many attribute of *sfes* are specific deficiencies in numerical discretization of the equations of motion, parameterizations of sub-grid processes, etc. In this report, we aim to estimate these models bias that leads to *sfes* in the period 2018-2019.

System forecast errors: July – August 2018

$$sfe = \overline{V_f} - \overline{V_t}$$

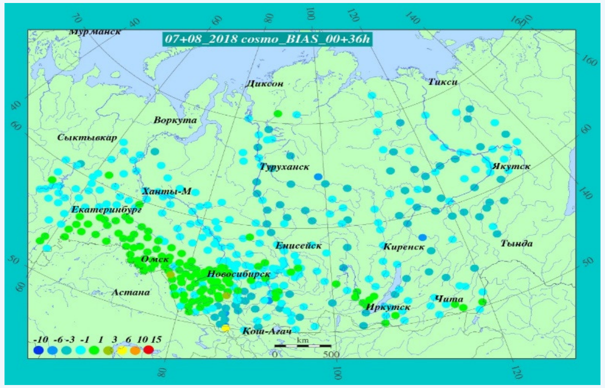

07+08_2018_cosmo_BIAS_36h

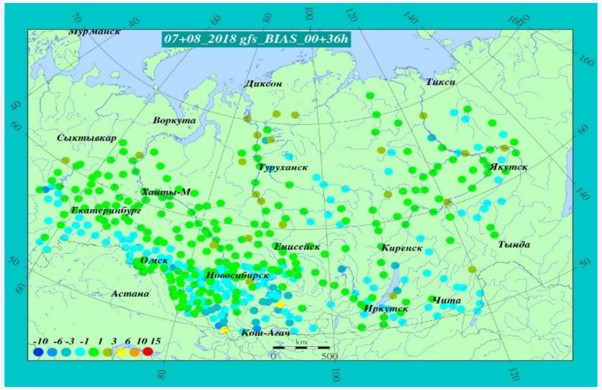

07+08_2018_gfs_BIAS_36h

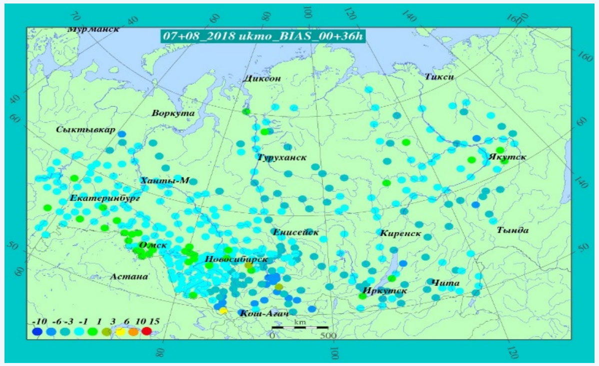

07+08_2018_ukmo_BIAS_36h

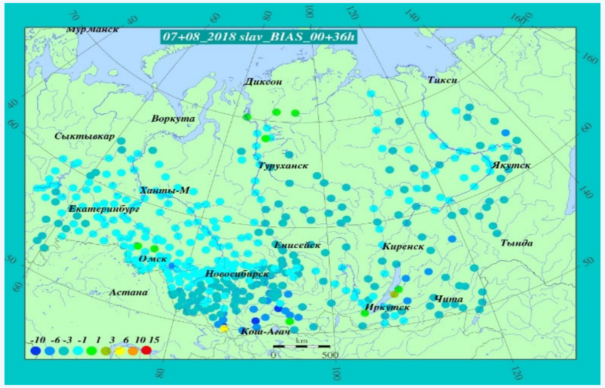

07+08_2018_slav_BIAS_36h

System forecast errors: December – February 2019

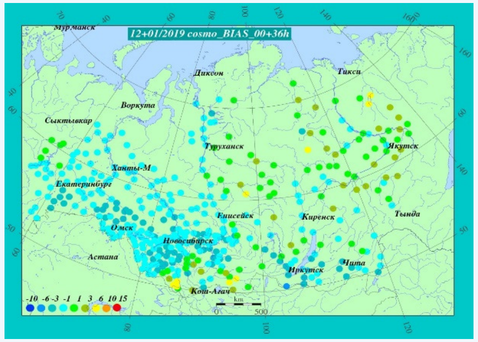

12+01_2019_cosmo_BIAS_36h

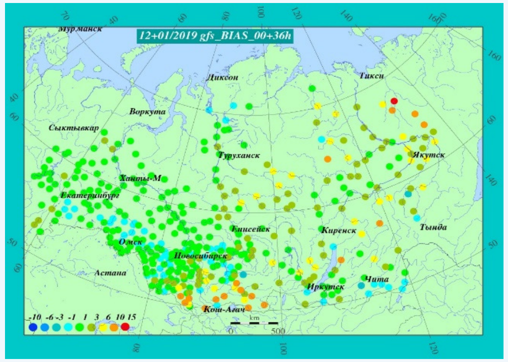

12+01_2019_gfs_BIAS_36h

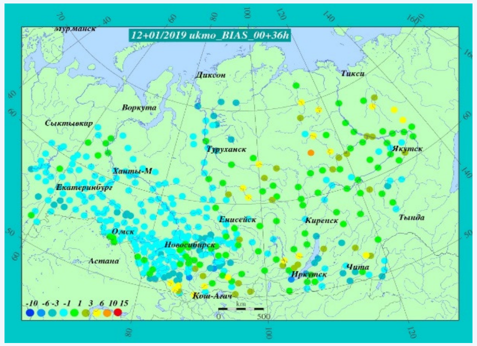

12+01_2019_ukmo_BIAS_36h

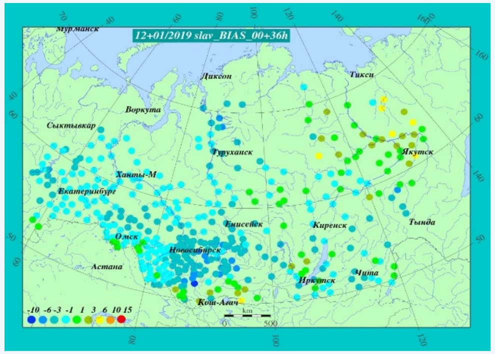

12+01_2019_slav_BIAS_36h

As a test, Earth Climate System model Plasim-ECS-ICMMG-1.0. was calculated for a period of 100 years. The initial state of the atmosphere was obtained in previous experiments with the full version of the stand-alone PlaSim model.

Surface air temperature and precipitation fields are plotted in Figures:

1. First figure shows the surface temperature, obtained as a result of averaging over the last 35 years of the experiment and over the 1979-1999 of the NCEP2 Reanalysis data for January and July;

    In general, the model surface temperature distribution is in good agreement with NCEP2 Reanalysis data, but some regions are overheated. It is about 5 degree warmer in central part of Eurasia in January, in southern part of this region in July, in western part of South America in January and in North America in both considered months. In Polar regions the model surface temperature lower than that is in Reanalysis data in its winter seasons (in January is for North Pole and in July is for South Pole) ⇨ **climate bias**

2. Second figure shows the total precipitation, obtained as result of averaging over the last 35 years of the experiment and over the 1979-1999 of the GPCP ver. 2.3 data (www.esrl.noaa.gov) for January and July,

    Model data shows a good agreement with the observation data, but it is about 10-15 mm per day more in modeling data then in observations in tropics for both considered months. Main arid regions are captured, as is the seasonal migration of the Inter-Tropical Convergence Zone and associated monsoon systems ⇨ **climate bias**

The average January and July climatology simulated by the PlaSim -_ICMMG-v.1.0 model and Reanalysis data for January and July

a)

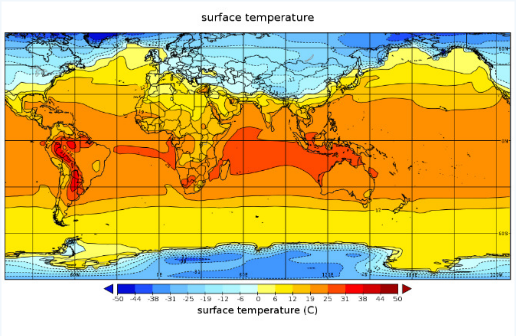

b)

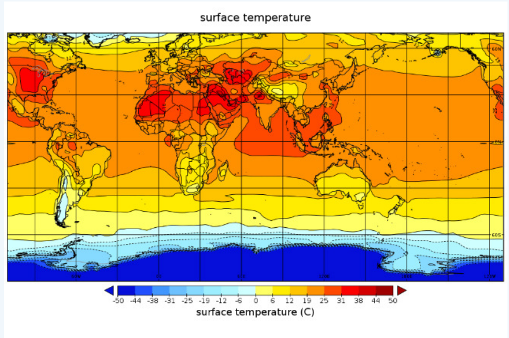

c)

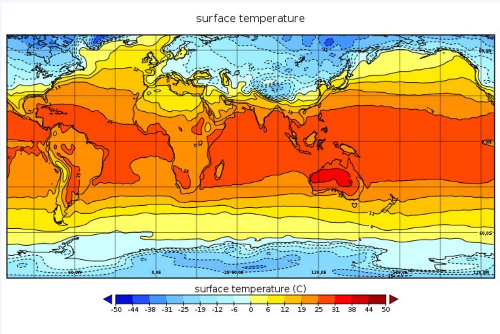

d)

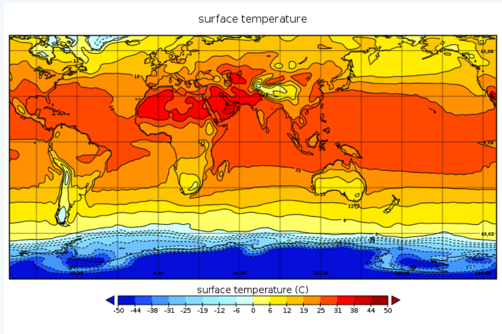

Surface temperature averaged over the last decade of the 100-year preliminary experiment: a) in January; b) in July. The climatological surface temperature for NCEP2 Reanalysis averaged over 1979-1999 for c) January and d) July.

Seasonal surface air temperature (C) difference: (PLASIM-ICMMGv.1.0 - NCEP) - a) January, b) July;
(PLASIM - NCEP) – c) January, d) July

a)

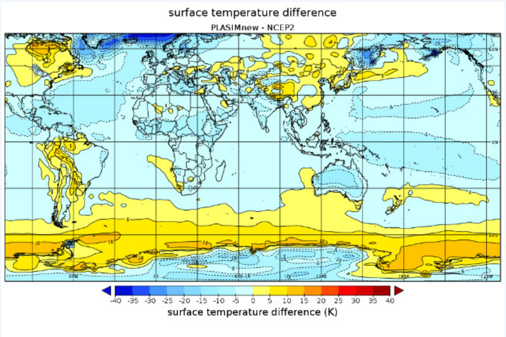

b)

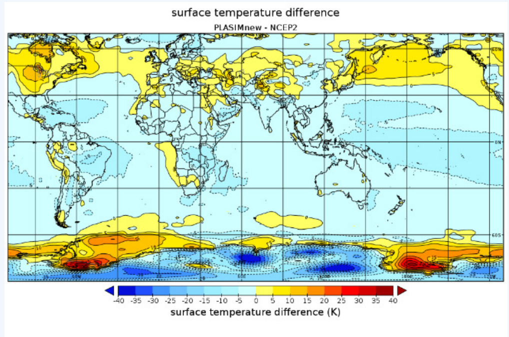

c)

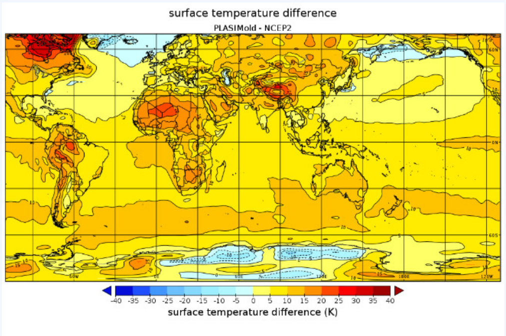

d)

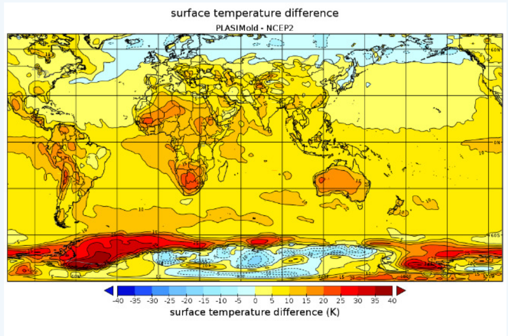

Combined precipitation averaged over the last decade of the 100-year preliminary experiment: a) in January; b) in July. The climatological total precipitation for GPCP ver. 2.3 dataset averaged over 1979-1999 for c) January and d) July (www.esrl.noaa.gov).

a)

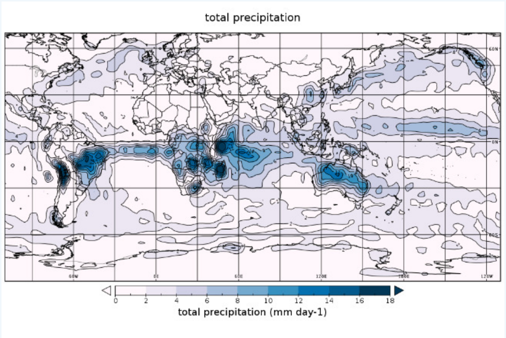

b)

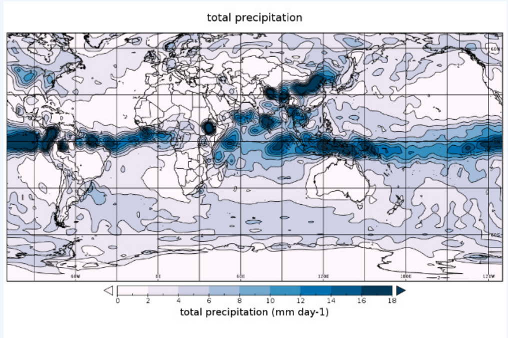

c)

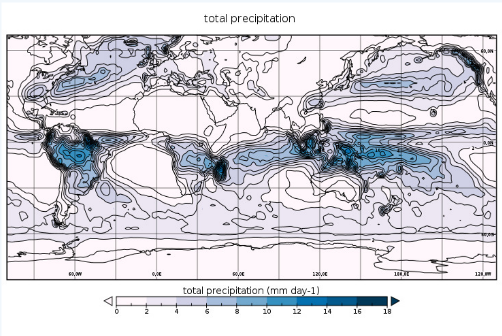

d)

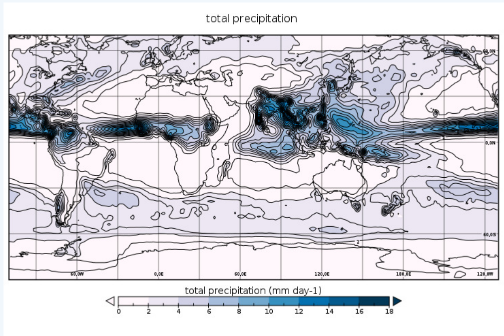

Differences between combined precipitation averaged over the last decade of the 100-year preliminary experiment and climatological total precipitation for GPCP ver. 2.3 dataset averaged over 1979-1999(www.esrl.noaa.gov): a) in January; b) in July for PlaSim-ICMMG-v.1.0 ; c) January and d) July for PlaSim

a)

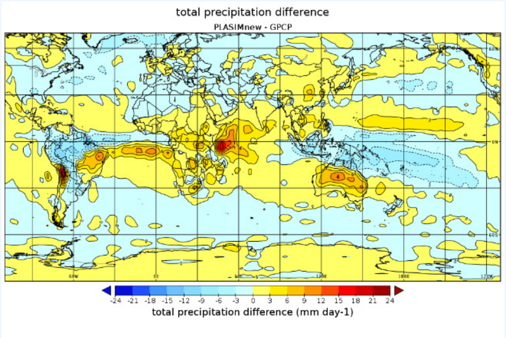

b)

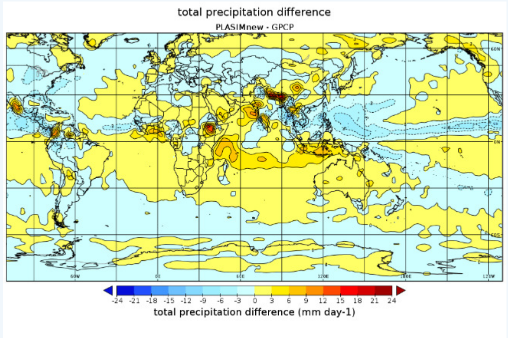

c)

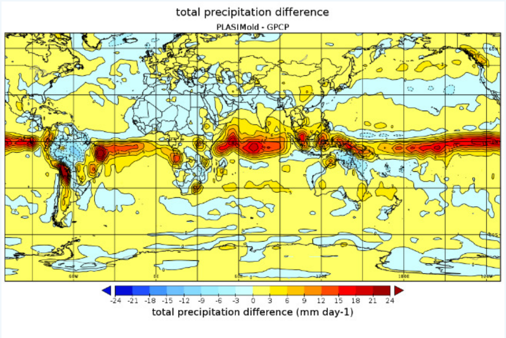

d)

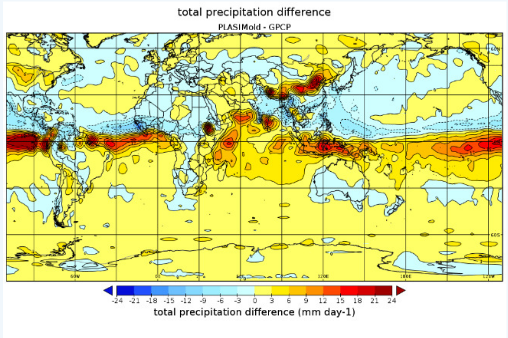

For extended forecast ranges, the mean error is almost constant and equal to the difference between model's climate and the observed climate (**climate drift-bias**). The fact that the spatial distribution of systematic errors in the medium range has large-scale features similar to the climate drift, indicates that those error components are mainly associated with deficiencies in model formulation (*L. FERRANTI, E. KLINKER, A. HOLLINGSWORTH and B. J. HOSKINS, 2002*).

2. Diagnosing the causes of bias in climate models – why is it so hard?

(T. N. PALMER and ANTJE WEISHEIMER, 2011)

Well known that systematic errors (biases) of a forecast model arise from different components of model physics and dynamics.

Whilst it is easy to identify these biases, it is another matter to determine the causes of these biases.

The Northern Annular Mode (NAM), or Arctic Oscillation (AO), (Thompson and Wallace 1998) corresponds largely to fluctuations in the zonal wind in the Northern Hemisphere.

We may be applied the fluctuation–dissipation theorem to understand the forced response of the atmosphere

(Leith, 1975; A. Gritsun and V. Dymnikov, 1999; A. Gritsun, et al.,2008; etc.)

$$\dot{X} = F(X), \quad \dot{X}^* = F(X^*) + \delta f$$

And $\delta X = X^* - X$, then fluctuation dissipation theorem states

$$\delta \overline{X} = L(\delta f)$$

where the overbar represents a long-time average and

$$L = \int_0^\infty C(\tau) C^{-1} d\tau$$

where C is the lag – τ covariance matrix of X

One can question whether the fluctuation–dissipation theorem holds quantitatively for a system like the atmosphere, far from equilibrium. Nevertheless, qualitatively we see in the fluctuation–dissipation theorem the notion that the response of a system to some prescribed forcing can be strongly conditioned by that system's internal modes of variability, i.e. the response to the forcing will be conditioned by the projection of δf in the direction of the leading eigenvectors of $\boldsymbol{L}$.

Additionally, given the non-self adjoint nature of $\boldsymbol{L}$, perturbations which optimally excite the leading eigenvector of L need not point in the direction of this eigenvector

Rossby Wave–Breaking and NAO/AO

The basic spatial and temporal structure of the large-scale modes of intraseasonal variability in the extratropical atmosphere is known to be represented by fairly well-defined patterns, and among the most prominent are the North Atlantic Oscillation (NAO) and a more zonally symmetric pattern known as an **annular mode (AO in NH)**. In article (Benedict et al., 2004) was suggested that wave-breaking process is responsible for the variations associated with the North Atlantic Oscillation (NAO). Benedict et al. (2004) identified “NAO events” on the synoptic time scale, concluding that the **breaking of upper-level Rossby waves was responsible for the NAO anomalies**, with anticyclonic breaking leading to a positive +NAO event and cyclonic breaking leading to a negative - - NAO event.

RELATIONSHIP BETWEEN **FORECAST ERRORS** AND **NAO/AO**

The NAO is an important mode of atmospheric variability and is related to the position and strength of the North Atlantic storm tracks. The NAO index is traditionally defined as the mean-sea level pressure difference between the Azores and Iceland. **The NAO is associated with changes in the location of storm tracks, regional anomalies in precipitation and temperature, large-scale sea surface temperature anomalies (SST).**

AO: PLASIM - 22.99 %   NCEP2(NOAA) - 20.81 %

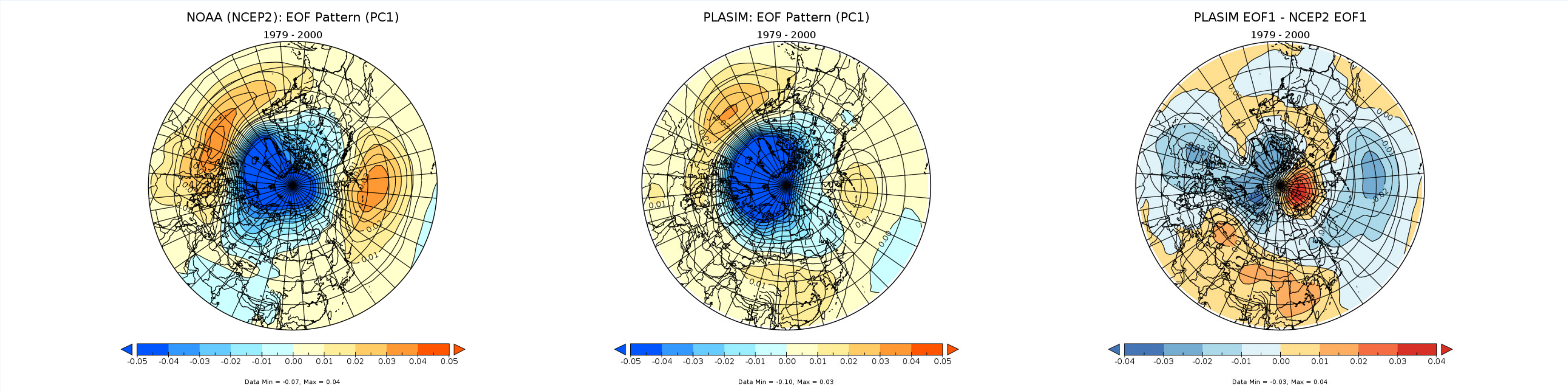

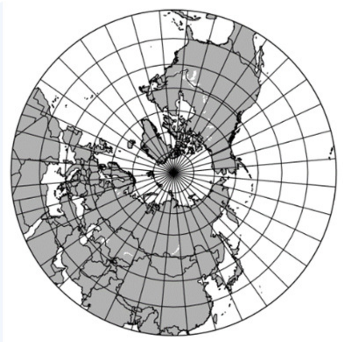

AO in ERA dataset, which explains 31.7% of the total variance; in MME (multimodel ensemble of 39 CMIP5 models), the variance explained by AO is 32.4%,

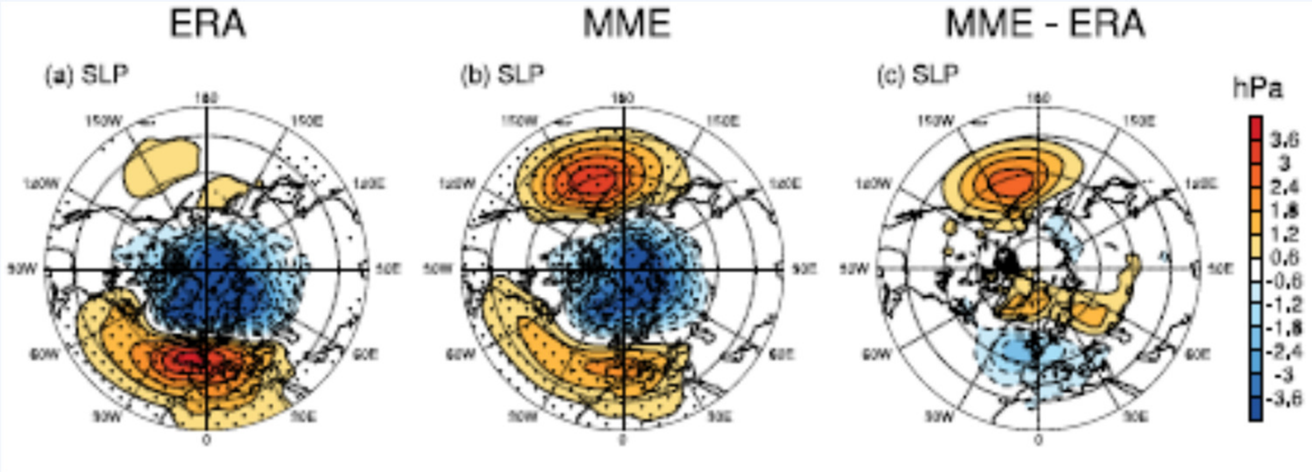

The winter mean SLP regressed on the normalized AO index in (a) ERA dataset and (b) MME for the period 1961–2005 (c) The difference between (b) and (a).

Rossby Wave–Breaking

Tropospheric mixing and transport in the middle and high latitudes are driven mainly by eddy activity. In many cases, eddies grow by baroclinic instability and decay barotropically by breaking and inducing irreversible mixing of the surrounding air, termed “wave breaking” [McIntyre and Palmer, 1983]

The Rossby waves breaking in the stratosphere has a significant impact on the dynamic fields in the troposphere. For example, in winter in extratropical latitudes, the manifestation of waves breaking are sudden stratospheric warming, which have a significant effect on the weather in the troposphere.

The breaking planetary waves will tend to erode the winter polar vortex by mixing pieces of it into the surrounding "surf zone". We have seen that corresponding mixing of extra-vortex air into the vortex is much weaker. Therefore the vortex will reduce in area but will not lose intensity. Opposing this will be diabatic effects, tending to restore the vortex to its "radiative equilibrium" structure.

The Rossby waves breaking in the stratosphere and their reflection in the troposphere have a significant impact on the dynamic fields in the troposphere.

An indicator of the instability of vertically propagating Rossby waves is the presence in the field of a potential vortex (PV) of **filamentary vortex structures (the so-called streamers),** as well as closed isolines, which can be sections of a polar vortex and isentropic surfaces. The PV isoline with a value of 2PVU determines the dynamic tropopause. Therefore, the formation of filamentary structures of the polar vortex can be interpreted as the penetration of the stratospheric air into the troposphere.

There are cyclonic and anticyclonic types of wave breaking. The type of wave breaking is determined by the sign of the potential vortex anomaly. The cyclonic type of breaking is characterized by streamer-shaped vortex structures extending to the equator from the main vortex. Anticyclonic and cyclonic breaking have different effects on atmospheric circulation..

We analyzed the fields of a PV = $Q = -g\left(\xi_p + f\right)\frac{\partial \theta}{\partial p}$ for data obtained ***using the Planet Simulator model of the general atmospheric circulation.***

To identify filamentary structures, the method proposed in the paper (***Wernli, H., M. Sprenger, 2007***) was used. Here the term stratospheric PV streamer/cutoff refers to stratospheric features on isentropic surfaces (PV > 2 PVU), and the term tropospheric PV streamer/ cutoff is used for their tropospheric counterparts (PV < 2 PVU).

a) three streamers

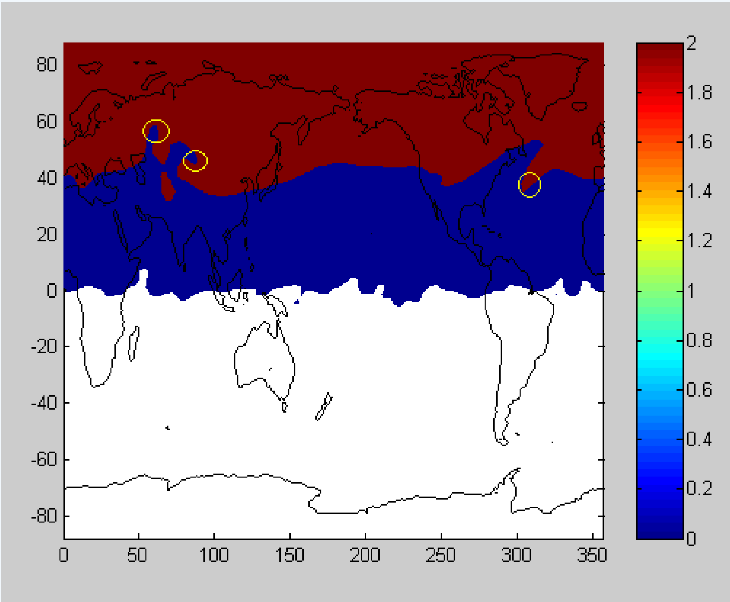

b) no streamers - all vortex structures are larger than a given scale

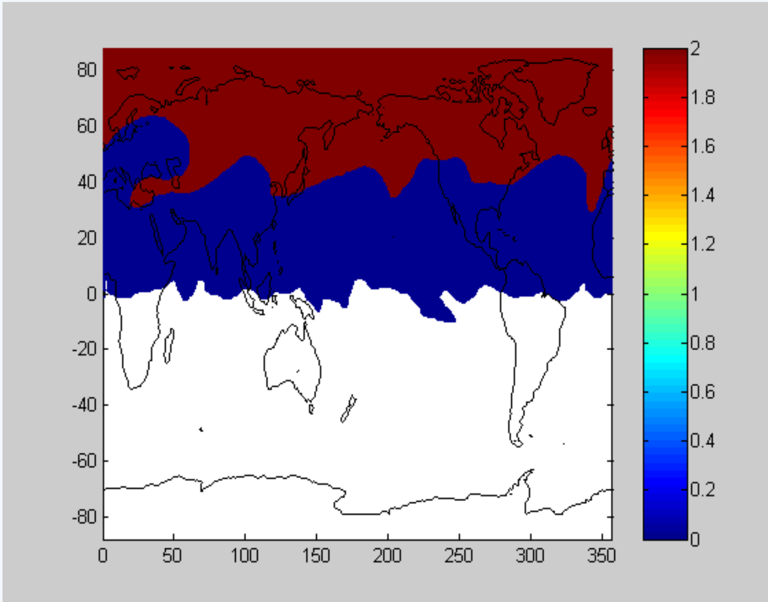

Schematic depiction of the streamer identification.

The black line corresponds to the 2PVU contour on an isentropic surface. The shaded region corresponds **to a stratospheric streamer** since the spherical distance d between two points of the contour is smaller than the threshold D and the distance along the contour connecting these points l is larger than the threshold value L.

Technically, for every pair of contour points it is checked whether

(i) the direct spherical distance between the two points d is smaller than a certain threshold distance ($d < D = 800$ km) and

(ii) the connection between the two points along the contour l is longer than a threshold ($l > L = 1500$ km), as illustrated in figure.

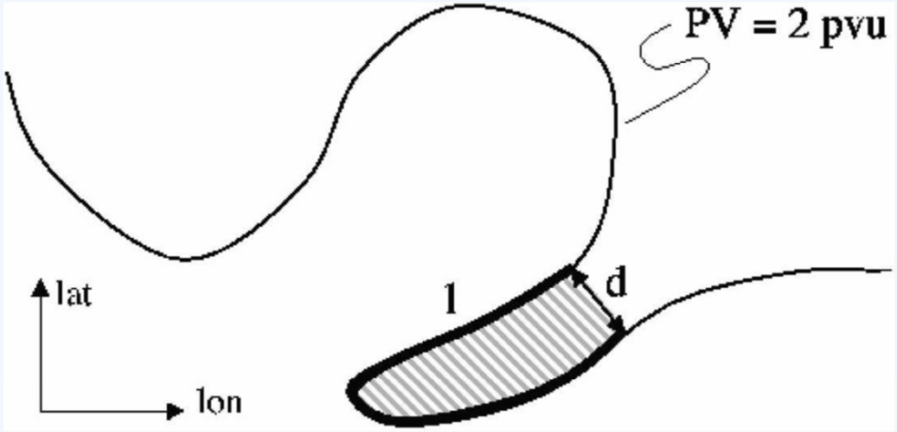

The main areas of instability were analyzed for different seasons of the year. The intersection of the surface

$$Q = 2PVU$$

with isentropic surfaces was considered. The isolines of a potential vortex with a value of 2PVU on different isentropic surfaces are shown in the figure. The average latitude of the isoline of the potential vortex decreases with increasing potential temperature. For values of 310-350K, the equivalent latitude is 50-30.

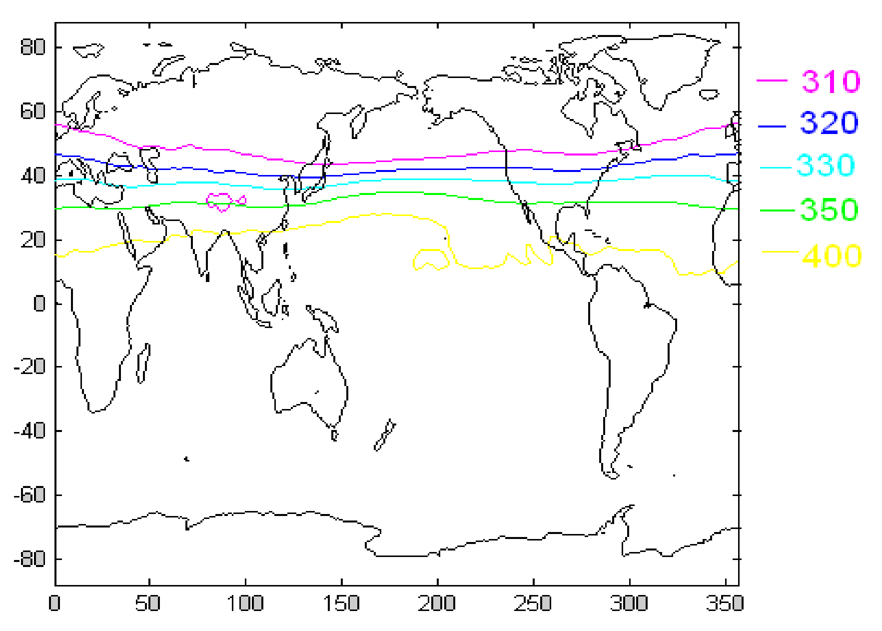

Isolines of a potential vortex with a value of 2PVU for various isentropic surfaces (January). Different colors indicate the potential temperature values to which the line corresponds

θ K	month	number of vortex structures			
		streamers, cyclonic anomaly	streamers, anticyclonic anomaly	sections, cyclonic anomaly	sections, anticyclonic anomaly
350	january	6	6	7	3
330	january	8	15	12	30
310	january	26	24	56	61
330	july	33	61	149	189
350	july	60	27	156	67

In the summer, a significant amount of vortex structures is observed at θ = 350 K and θ = 330 K, with streamers with anticyclonic dominating at θ = 330 K and with cyclonic anomaly at θ = 350 K. Thus, in the summer, in the region lying between the isolines θ with values of 330 and 350K, there is an active mixing of air masses. This area is located at 40-50 north latitude.

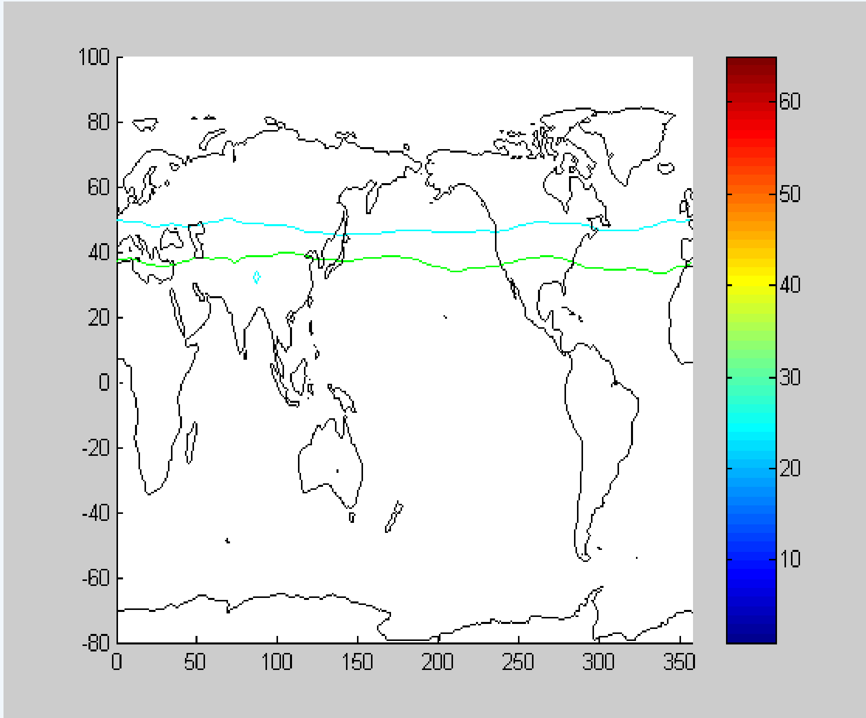

Isolines of potential temperature with values of 330 K (blue line) and 350 K (green line) on the surface Q = 2PVU in July.

Atmospheric blocking as a midlatitude weather pattern usually **occurs following the breaking of a Rossby wave** at the exit of the storm track, when a subtropical low-vorticity air mass is advected poleward developing an anticyclonic circulation.

- It is important to note that numerical models have been shown to have limited skill in reproducing blocking. It was discovered that bad forecast of blocking accounted for a **large part of the systematic error** of numerical weather prediction (Tibaldi et al. 1994, etc.).

- This poor skill is noted for general circulation models used for climate purposes.

- Even the more recent analyses from the Coupled Model Intercomparison Project (Anstey et al. 2013; Masato et al. 2013, etc.) still suggest the presence of **a negative bias** especially over Europe.

Winter Arctic warming and its linkage with midlatitude atmospheric circulation and associated cold extremes: The key role of meridional potential vorticity gradient.
2019 Science China Earth Science. **Muyuan LiDehai Luo**

The surface air temperature over the Eurasian continent has exhibited a significant cooling trend in recent decades (1990–2013), which has occurred simultaneously with Arctic warming and Arctic sea ice loss. While many studies demonstrated that midlatitude cold extremes are linked to Arctic warming and Arctic sea ice loss, some studies suggest that they are unrelated. The causal relationship between midlatitude cold extremes and Arctic change is uncertain, and it is thus an unsolved and difficult issue. It has been widely recognized that the severity and location of midlatitude cold extremes are closely related to the persistence, location and movement of blocking systems. It might be possible that the Arctic sea ice decline or the Arctic's warming influences midlatitude cold extremes by changing the blocking system.

This paper reviews the recent research advances on the linkages between the blocking system and Arctic warming. The nonlinear multiscale interaction model of Luo et al. revealed that the magnitude of the meridional gradient (PVy) of the background potential vorticity (PV) is a key parameter that reflects changes in the dispersion and nonlinearity of the blocking system. It was found that Arctic warming played a role in reducing the dispersion of the blocking system and enhancing its nonlinearity by reducing the magnitude of PVy. A small PVy is a favorable background condition for increasing the duration of blocking events and producing midlatitude cold extremes. However, because the magnitude of PVy reflects the difference between the background PV of the Arctic high latitudes and the midlatitude continent, the occurrence of midlatitude cold extremes not only depends on an anomalous background PV over Arctic high latitudes but also on its value over the midlatitudes. Thus, Arctic warming or sea ice decline is not necessary for the occurrence of midlatitude cold extremes.

Processes in Clouds Influence Large-Scale Precipitation Variability and Extremes

To accurately simulate and predict precipitation, particularly when it is extreme, it is critical to understand how in-cloud microphysical processes, such as condensation of vapor and evaporation of rain and cloud particles, cascade up to influence large-scale precipitation variability. However, because these influences are non-linear and cross a broad range of spatial scales, arriving at this understanding is challenging.

Using high-resolution modeling with theoretical and statistical analysis, a research team led by scientists at the U.S. Department of Energy's Pacific Northwest National Laboratory revealed a direct link between the in-cloud processes and the frequency of precipitation extremes. Their findings led to a new approach for using observations to constrain the representation of cloud microphysical processes in Earth system models.

CONCLUSIONS AND WAYS FORWARD

Despite advances in resolution and development of models in recent years (E. Volodin et al., 2017; I. Esau, M. Tolstykh, et al., 2018, etc.), due to enhanced computer power, numerical weather prediction and climate models still needs parameterizations of diabatic processes and will continue to do so for the near future. These parameterizations introduce inaccuracies into models and contribute to the occurrence of systematic forecast error.

The reduction of systematic errors permit us:

(i) extended accurate lead times for numerical weather prediction forecasts,

(ii) improved lateral boundary conditions for high-resolution domains nested within global models, and

(iii) improved statistical properties of climate integrations.

Climate models and physical parametrization in terms of the symmetry properties of a system of equations (again).

What processes should be parameterized?

Physics models include:

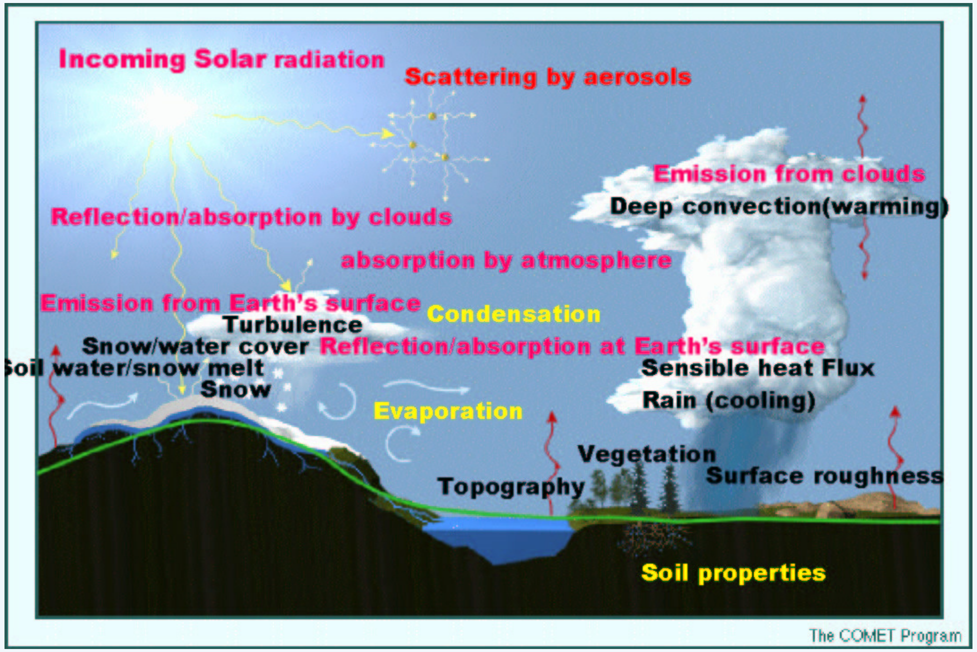

Conservative parameterization schemes

(A. Bihlo and G. Bluman, 2012)

- The problem of replacing the continuous governing equations of the atmosphere–ocean system by a discrete approximation is that in general no numerical scheme is capable of preserving all the geometrical features that the initial system of differential equations possesses**. Among these features are symmetries and conservation laws.**

$$L_l(x,u^{(n)})=0,\ l=1,\ldots,m;\quad x=(x_1,\ldots,x_p),\quad u=(u_1,\ldots,u_q)$$

n-maximum order of derivatives included in the system

Transformations are generated by infinitesimal operators.

$$X=\sum_1^p \xi_i(x,u)\frac{\partial}{\partial x_i}+\sum_1^q \eta_j(x,u)\frac{\partial}{\partial u_j}$$

$(x,u) \longrightarrow$ n-continuation space

$$L_l(x, u^{(n)}) = 0,\ l = 1, \ldots, m; \qquad x = (x_1, \ldots, x_p), \quad u = (u_1, \ldots, u_q)$$

$$\Downarrow$$

$$u = \bar{u} + u', \quad \rightarrow \quad \tilde{L}_l(\bar{x}, \bar{u}_{(n)}, w) = 0 \qquad (*)$$

w includes all averaged non-linear combinations of terms, which cannot be obtained using quantities

$$\overline{u}^{(n)}$$

Such combinations typically include, for example, members of this type:

$$\left(\overline{u'v'}\right), \left(\overline{u'\overline{u}}\right), \left(\overline{u'u'_x}\right)$$

Which belong to the subgrid processes.

To solve the system (*), appropriate assumptions about w must be made.

$$\tilde{L}_l(\overline{x}, \overline{u}_{(n)}, f(x, \overline{u}_{(r)})) = 0, l = 1, \ldots, m$$

(**)

$$w = f(x, \overline{u}_{(r)}),\ f = (f^1, \ldots, f^k),$$

If the choice of the functions f = (*f1, ..., fk*) is made within the framework of the preservation of symmetries, where k is the number of "unclosed" members that must be parameterized, for this you need to perform a group analysis of the system (**).

The formulation of the “correct” dimension parametrization scheme is a simple task, but not all schemes that are used in practice are invariant, for example, with respect to the Galilean transformation. An example is the classical Kuo scheme for deep convection. The basis of this scheme is the assumption that the convergence of moisture in the lower layer is proportional to the intensity of precipitation. The intensity of precipitation is invariant with respect to the Galilean group, and the convergence of moisture does not possess this property, those. The Kuo scheme does not have the symmetry property, which can lead to

non-physical effects when modeling climate.

↓

global and regional climate models are biased

Thank you to all the CITES-2019 members